Numerical Investigation and Optimization of Pyrolysis Process: Effects of Viscous Models and Combustion Power on Fluid Dynamics and Heat Transfer

Rouf Muhammad[1*], *Hamid Ramadhan* Nur[2], *B. S. Rahayu* Purwanti[3], *Muhammad* Nurtanto[4], *Ghani Putra* Nuari[5], *Muhamad Fajar* Ramadhan[6], and *Ainur Nurkalyevna* Berkinbayeva[7]

[1, 2, 6]Department of Mechanical Engineering, Politeknik Negeri Jakarta PSDKU Demak, 59516 Central Java, Indonesia
[3, 5]Department of Electrical Engineering, Politeknik Negeri Jakarta, 16425 Depok, West Java, Indonesia
[4]Department of Vocational Technology and Education, Universitas Negeri Jakarta, 13220 Jakarta, Indonesia
[7]Institute of Metallurgy and Ore Beneficiation, Satbayev University, 050010, Kazakhstan

Abstract. The combustion of pyrolysis oil in industrial gas turbines utilizing biofuel represents a renewable energy source that originates from biomass waste. This combustion process presents a viable alternative to fossil fuels in industrial applications, contributing to a decrease in carbon emissions and mitigating greenhouse gas effects. An analysis of thermal and hydrodynamic factors is essential for comprehending how different combustion capacities and pyrolysis geometries like length, width, and storage volume affect system performance. This study aims to investigate how different variations of the k-ω viscosity model (k-ω Standard, SST, GEKO, and BSL) affect the pyrolysis combustion process of a gas-fired industrial burner with capacities of 200 kW, 700 kW, and 1000 kW. Numerical studies employing computational fluid dynamics (CFD) were carried out to ascertain the optimal thermal and hydraulic performance. The findings indicate that the k-ω standard viscous model produces the most favorable outcomes, with SST, GEKO, and BSL following closely, evaluated on parameters including air flow rate, maximum wall temperature, coefficient of heat transfer, and Nusselt number. Therefore, the k-ω standard numerical model, which has a combustion capacity of 1000 kW, is applicable for the geometric calculations of various pyrolysis gas-fired industrial burners.

* Corresponding author: rouf.muhammad@mesin.pnj.ac.id

© The Authors, published by EDP Sciences. This is an open access article distributed under the terms of the Creative Commons Attribution License 4.0 (https://creativecommons.org/licenses/by/4.0/).

1 Introduction

Pyrolysis oil combustion in industrial gas turbine biofuel applications is a renewable energy source derived from biomass waste materials[1]. Pyrolysis oil combustion has significant potential as an alternative fuel to replace fossil fuels in practical industrial applications[2]. This type of fuel provides a basis for reducing carbon emissions and mitigating greenhouse gas effects in the industrial sector[3]. Therefore, optimizing pyrolysis combustion for waste treatment is a key priority[4]. However, waste is a potential energy source that needs to be harnessed and developed further to benefit the environment and reduce dependence on fossil fuels[5,6]. Generally, some waste cannot be processed or recycled due to its excessive pollution effects, necessitating environmentally friendly methods like waste-to-electricity (WTE) conversion[7]. This WTE conversion process can be achieved through pyrolysis technology[8]. In this context, pyrolysis oil combustion and pyrolysis gas-fired industrial burners are well-suited for addressing this issue[9].

To optimize the performance of pyrolysis gas-fired industrial burners, both experimental and numerical research is necessary[2]. Experimental methods have been extensively developed among researchers with various parameters, including combustion capacity, geometric variations such as length, width, and pyrolysator storage volume, as well as combustion ignition[3,8,9]. However, numerical research utilizing Computational Fluid Dynamics (CFD) software has emerged as a viable approach to optimize the performance of pyrolysis gas-fired industrial burners[10][11]. Simulations using numerical methods in Computational Fluid Dynamics (CFD) software for pyrolysis gas-fired industrial burners offer several advantages, including cost savings, reduced physical property requirements, and enhanced efficiency and effectiveness[12]. Experimental and numerical studies on natural gas combustion pyrolysis reactors aim to produce acetylene gas for engineering applications. This research proposes the Reynolds-Averaged Navier-Stokes (RANS) and Large Eddy Simulation (LES) models. The results indicate that the RANS model can generate 1177 m^3/h of natural gas and produce 2.5 kTA of acetylene gas[13].

The k-ω and k-ε turbulence models were employed in a numerical study to investigate the thermal load and NO emissions of a novel 1 MW pyrolysis gas/natural gas-fired industrial burner. The results showed that the k-ω model worked better, producing a steady flame without backfire when the burner was adjusted from 200 kW to 1000 kW, even with about 10% H_2 in the pyrolysis gas. Additionally, both natural gas and pyrolysis gas can be used as main fuels at low and high power levels, staying within the NO emission limit of 250 mg/Nm^3 and reaching the temperature requirement of 1400°C[9]. The volume-averaged Navier-Stokes equations and Eulerian grids were utilized for grid generation and coupled with the Spalart-Allmaras and Reynolds Stress turbulence models in a numerical investigation of biomass pyrolysis in a draft-tube spouted reactor with a fountain confiner. The results showed that using the Spalart-Allmaras model made combustion more efficient by 14.8%, indicating it could be a good choice for computer simulations of biomass pyrolysis in similar reactor setups[14].

The study used inviscid and laminar flow models in a CFD-based numerical analysis of iron-coke briquette pyrolysis and reduction. The results indicated that the combustion performance and heat transfer coefficients exhibited similar trends, with a deviation of around ±12%[15]. Prior research has primarily focused on characterizing viscous models for numerical analysis of thermal and hydrodynamic performance in pyrolysis systems, considering factors such as combustion capacity and geometric variations. However, the impact of different k-ω turbulence models (Standard, SST, GEKO, and BSL) on pyrolysis gas-fired industrial burners with varying combustion capacities (200 kW, 700 kW, and 1000 kW) remains unexplored. This study aims to address this gap by investigating the effects of

these models on thermal and hydraulic performance using computational fluid dynamics (CFD) simulations.

2 Method

2.1 Physical Model and Computational Domain

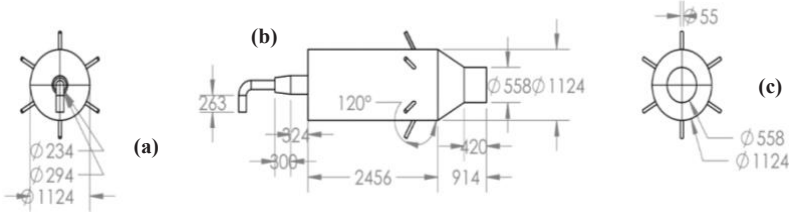


Fig. 1. (a) Top View, (b) Side View, and (c) Bottom View.

Figures 1(a), 1(b), and 1(c) show the top, side, and bottom views of the pyrolysis gas-fired industrial burner, along with its dimensional specifications. The pyrolysis gas-fired industrial burner was modeled using SolidWorks software, based on the literature [9], with the detailed component arrangement shown in Figure 2.

The computational domain is defined using the Design Modeler menu within the Computational Fluid Dynamics (CFD) software. The computational domain size is referenced in the literature [9]to examine the characteristics and behavior of multiphase flow, as well as thermal and hydraulic properties in the pyrolysis gas-fired industrial burner. This analysis assumes steady-state conditions while incorporating the differential mathematical equations of continuity, momentum, and energy established in the numerical study. The equations for continuity, momentum, and energy in the numerical analysis of the pyrolysis gas-fired industrial burner are expressed as follows:

The continuity equation, which delineates the variation of a specific quantity in relation to space and time, is expressed as:

$$\frac{\partial \rho}{\partial t} + \nabla(\rho u) = 0 \tag{1}$$

In this case, ρ represents the fluid density, t equates to the time variable, ∇ means the nabla operator, and u = (u, v, w). T indicates the velocity of the continuous phase of the gas mixture within the Cartesian coordinate system. The Navier-Stokes equations incorporate momentum conservation, with the momentum equation expressed as follows:

$$\frac{\partial(\rho u)}{\partial t} + \nabla(\rho u u) = \rho g - \nabla p + \nabla \tau = 0 \tag{2}$$

Let g represent the gravitational acceleration vector, p indicate the static pressure, and τ signify the stress tensor. The energy equation expressed in terms of specific enthalpy (h) is represented by the following formula:

$$\frac{\partial(\rho h)}{\partial t} + \nabla(\rho u h) - \nabla\left(\frac{k}{Cp}\nabla h\right) = Sh \tag{3}$$

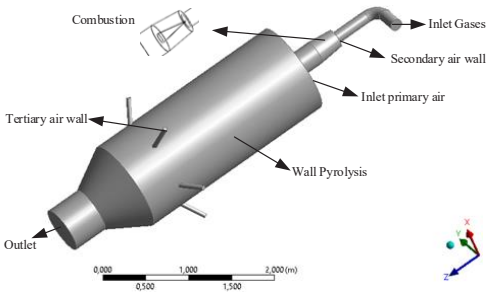


Fig. 2. Computational Domain of Pyrolysis Gas-Fired Industrial Burner.

2.2 Meshing

The application of a control volume-based technique for meshing is employed to discretize the differential equations utilizing a first-order upwind scheme, enhancing accuracy and yielding improved results in the numerical study process. A fully structured Poly-Hexcore Grid mesh with high resolution is utilized near the walls in the computational domain to effectively capture the thermal and hydraulic boundary layer effects, as shown in Figure 3. Face sizing is utilized to establish acoustic mesh dimensions, determined at a measurement of 50 mm.

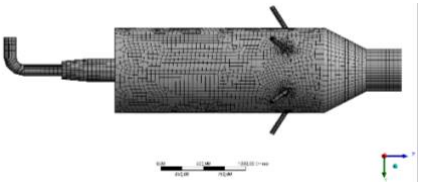


Fig. 3. *Poly-Hexcore Grid Structural*.

2.3 Simulation Set Up

The computational domain modeling of the pyrolysis gas-fired industrial burner is shown in Figure 2, which is based on experiments David, C., et al., [9]. The multiphase fluid flow is assumed to be steady with constant thermal physical properties. Convective heat transfer between the interface and fluid is considered. The convergence criteria used are 10^{-3} for flow and 10^{-5} for energy. The free fluid properties include a density of 1.196 kg/m³, a specific heat capacity of 1003 J/kg.K, a viscosity of 1.82×10^{-5} kg/ms, a thermal conductivity of 0.024 W/m.K, and a molecular weight of 28.966 kg/kmol. The operating conditions include an ambient temperature of 300 K, emissivity of 0.9, pressure of 100500 Pa, and a heat transfer coefficient of the burner wall of 5.5 W/m².K.

2.4 Grid Testing and Validation

To ensure the accuracy of numerical results, a grid independence test is conducted on the computational domain of the pyrolysis gas-fired industrial burner, as shown in Figure 4 (a). This test aims to determine the optimal point of experimental values based on the average wall surface temperature. The Grid Independent Test is performed with four variations of cell mesh numbers: 53344, 100625, 159469, and 208951. The test results show that the 159469 grid is suitable for use because the difference with the 208951 grid is relatively small (±0.2%) in terms of wall surface temperature values.

We performed validation using a numerical approach against experiments conducted in the literature [9] on a pyrolysis gas-fired industrial burner. The parameters investigated in this research include the average wall temperature of the pyrolysis gas-fired industrial burner, which is used to calculate the heat transfer coefficient and Nusselt number, as well as the average air volumetric flow rate, which helps determine the ideal gas composition in the newly proposed burner. We carried out the validation by varying the grid number in relation to the power combustion value of the pyrolysis gas-fired industrial burner. Figure 4 (b) shows the validation results, illustrating the relationship between volumetric flow rate and power combustion. The tests done by David et al. (2025) [9] on a pyrolysis gas-fired industrial burner showed flow rates of 200 m³/h, 700 m³/h, and 1000 m³/h. In contrast, the simulation results yielded values of 258.660 m³/h, 749.860 m³/h, and 1072.324 m³/h. The largest relative error was 3.7% when comparing the experimental value of 200 m³/h to the simulated value of 258.660 m³/h, while the smallest relative error was 2.9% when comparing 700 m³/h to 749.860 m³/h. These results demonstrate a satisfactory agreement between the experimental study [9] and the numerical simulation being validated.

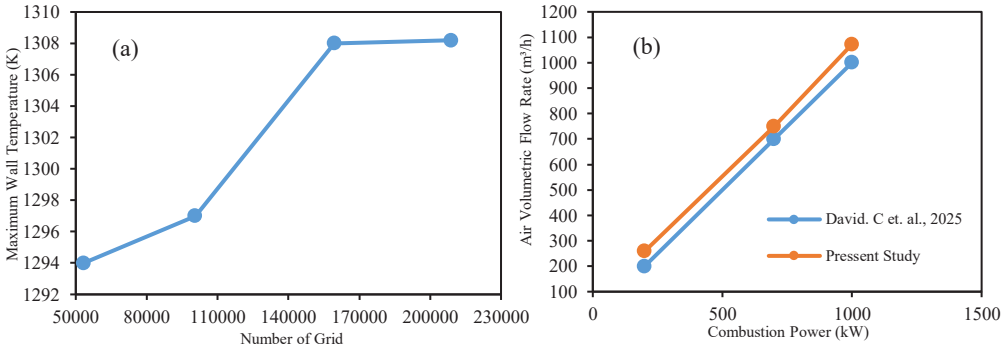


Fig. 4. (a) Testing Grid, (b) Validation

3 Result and Discussion

3.1 The Effect of Viscous K-*ω* Model

Optimization of pyrolysis gas-fired industrial burners is conducted by varying viscous models to find the optimal design and combustion capacity. Assuming constant heat flux, variations in viscous models and combustion power affect the heat transfer coefficient. Previous research David, C., et al., [9] shows that combustion power influences secondary air volumetric production, which can reduce NO gas emissions by up to 50%. Numerical studies show consistent results, with viscous model variations affecting air volumetric flow rate and maximum wall temperature in steady-state conditions. Viscous model variations also affect the heat transfer coefficient around the burner wall.

In the numerical analysis of pyrolysis gas-fired industrial burners, the k-ω standard viscous model shows the best performance, followed by the SST, GEKO, and BSL models. The k-ω standard model provides the best performance data with good numerical study convergence, enabling more accurate analysis. However, changes in the viscous model can affect important parameters such as air volumetric flow rate and maximum wall temperature. The temperature distribution in the k-ω standard model is sharper and more uniform compared to the GEKO and BSL models, demonstrating the superiority of this model in describing thermal phenomena. The results of numerical studies on various k-ω viscous models with a combustion power of 200 kW are shown in Figure 5 (a) which provide a more detailed picture of the temperature distribution in the pyrolysis gas-fired industrial burner.

The temperature distribution surrounding the pyrolysis gas-fired industrial burner exhibits significant variability, starting at a low of 300 K at the inlet and rising to between 1200 and 1400 K in the central region of the burner. The k-ω Standard and SST viscous models demonstrate a consistent temperature distribution, whereas the GEKO and BSL models exhibit a reduced temperature range of 1000-1200 K. Changes in the viscous model influence critical parameters, including air volumetric flow rate and maximum wall temperature, which in turn affect NO gas production. The results of the numerical study are given in Table 1 to show the impact of the viscous model on the heat transfer coefficient, Nusselt number, and air volumetric flow rate.

Numerical studies show that the k-ω standard viscous model performs best in calculating the maximum wall temperature in pyrolysis gas-fired industrial burners. The highest maximum wall temperature is obtained with the k-ω Standard model at a combustion power of 1000 kW, while the lowest value is obtained with the k-ω BSL model at a combustion power of 200 kW. The k-ω standard model is recommended for practical applications due to its high accuracy and stability. Maximum wall temperature affects the heat transfer coefficient and the quality of pyrolysis products. The pyrolysis process involves several phases with different temperature changes, namely drying, pyrolysis, and gas evolution. An optimal heat transfer coefficient ensures that the products produced have good quality. The distribution of heat transfer coefficients in pyrolysis gas-fired industrial burners can be seen in Figure 5 (b), which shows the difference in heat transfer coefficient distribution for various k-ω viscous models with a combustion power variation of 200 kW.

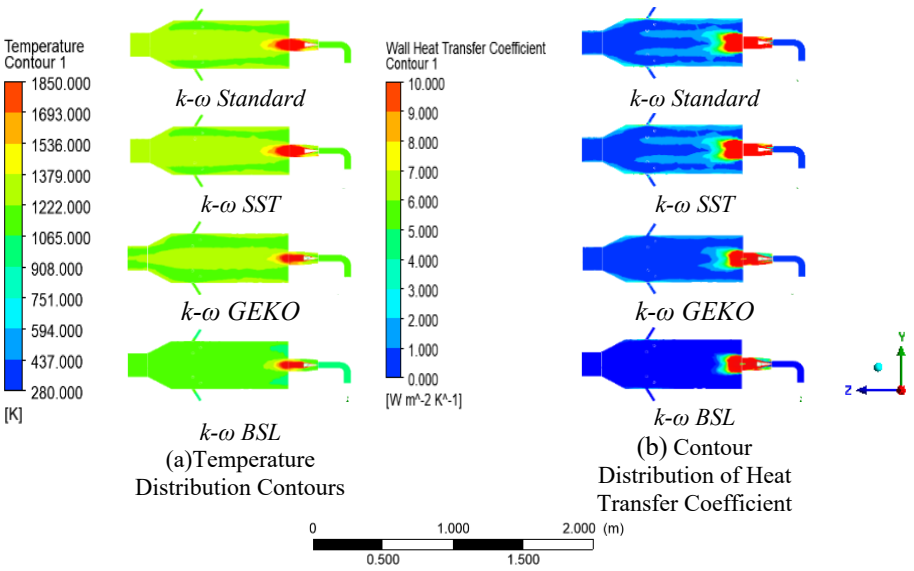


Fig. 5. (a)Temperature Distribution Contours and (b) Contour Distribution of Heat Transfer Coefficient on Pyrolysis Gas-Fired Industrial Burner Using Various k-ω Viscous Models with 200 kW Combustion Power Variation.

The heat transfer coefficient in pyrolysis gas-fired industrial burners is influenced by combustion power and viscous model variation. The greater the combustion power, the larger the heat transfer coefficient. The k-ω Standard and SST viscous models have a similar distribution of heat transfer coefficients, with values ranging from 3.84 to 20.90 W/m²K. The distribution of heat transfer coefficients tends to differ for each viscous model. As shown in Figure 5 (b) the distribution of heat transfer coefficients accumulates around the burner and

combustion chamber due to the combustion process effect. However, the k-ω GEKO and BSL viscous models have a thin distribution of heat transfer coefficients and do not show a distinct thermal boundary layer. This result affects the production of air volumetric flow rate and NO gas at 3% O_2.

3.2 The Effect of Combustion Power

This research characterized the combustion power of the pyrolysis gas-fired industrial burner using various k-ω viscous models. Combustion powers of 200 kW, 700 kW, and 1000 kW were proposed to characterize essential parameters including air volumetric flow rate (m^3/h), maximum wall temperature (K), Nusselt number, and heat transfer coefficient (W/m^2K). This study indicates that airflow characteristics decreased due to obstruction from the large flow field of the burner and combustion chamber, leading to minimal fluid movement through the gaps. The geometry of the burner and combustion chamber likely induced impact and collision forces, resulting in reverse flow in these areas.

The flow subsequently developed swirl characteristics and irregular vortex formations around the burner and combustion chamber. Subsequent to traversing the burner and combustion chamber, the flow exhibits a stable tendency devoid of boundary layer instabilities. Furthermore, we presume that the flow adjacent to the walls adheres to a no-slip requirement in this analysis. Consequently, the viscous k-ω model employed in this numerical investigation is highly suitable, as it can precisely discern the transitional flow features inside a cross-section. Table 1 shows that the markedly variable volumetric flow rates of water, differing by approximately 1 m/s, substantially influence the formation of NO gas at 3% oxygen. Furthermore, the combustion power effect demonstrates an enhancement in the streamlined flow and pressure along the walls of the gas-heated industrial combustion chamber. Figure 6 (a) shows the contour of the pressure distribution evolving on the geometry of the gas-heated industrial combustion chamber under different viscous model adjustments. The investigation of perpendicular forces on the hydraulic parameters surrounding the geometry of the gas-fired industrial burner revealed that the magnitude of combustion power and fluctuations in the viscous k-ω model pressure distribution are significant factors in this context. The surface area of the gas-fired industrial burner, the fluid type, the temperature, and the combustion volume and power yield diverse pressure behavior characteristics. Initially, low-pressure fluid enters from the input of the pyrolysis gas-fired industrial burner.

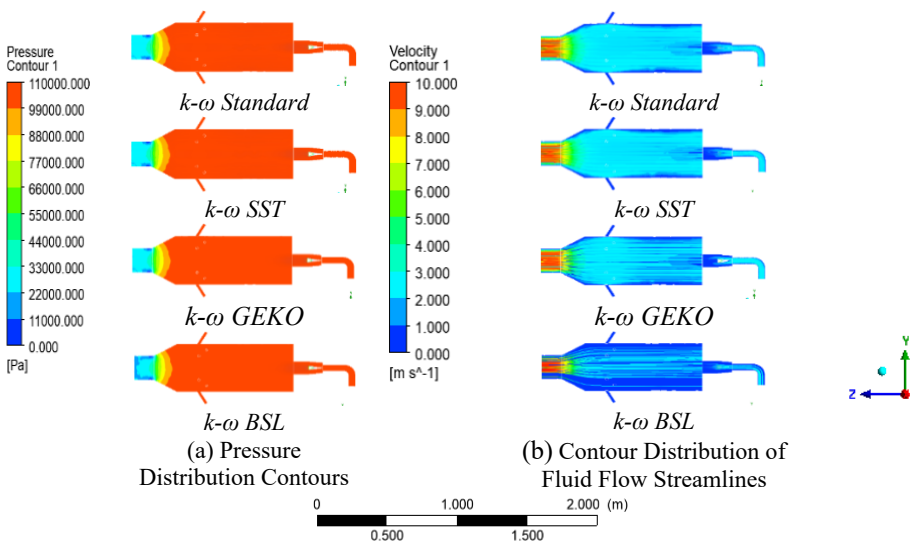
The pressure typically increases markedly in the vicinity of the burner and combustion chamber. This is due to the elevated temperatures in the burner and combustion chamber domains. Consequently, high pressure is uniformly spread throughout the whole surface of the pyrolysis gas-fired industrial burner. Boundary layer disturbances, such as surface roughness on the wall of the pyrolysis gas-fired industrial burner, result in a stable pressure distribution around the burner. The pressure ranges from 100500 Pa to 110000 Pa in the vicinity of the pyrolysis gas-fired industrial burner geometry. Nonetheless, paradoxically, the pressure progressively diminishes as the fluid nears the outflow region. This results from the influences of frictional force and substantial variations in flow velocity in the outflow region. Consequently, the values of the heat transfer coefficient and the Nusselt number diminish. Table 1 shows the characteristics from the numerical analysis of the pyrolysis of a gas-fired industrial burner, specifically the heat transfer coefficient and the Nusselt number.

The variation in fluid pressure generated in the gas-fired industrial burner during pyrolysis leads to minimal values of the Nusselt number parameter and heat transfer coefficient observed in the numerical analysis. The constant fluid flow rate's magnitude does not exert a considerable influence. The alteration in the viscous model throughout the numerical investigation led to a notable variation in pressure distribution. The k-ω GEKO and BSL viscous models exhibit significant pressure differences (ΔP) across various

combustion power levels. The observed pressure leads to a reduction in the Nusselt number and heat transfer coefficient by approximately 4%. The pressure drop observed at different combustion power levels in the case study for the numerical analysis of the pyrolysis gas-fired industrial burner results in a decline in these critical parameters, consequently diminishing the volumetric flow rate of water and gas NO at 3% O2 production. Figure 6 (b) shows the contour streamline of fluid flow evolving within the domain of the pyrolysis gas-fired industrial burner, considering different variations of the viscous model.

Table 1. Results of the Numerical Study in the form of Maximum Wall Temperature (K), Air Volumetric Flow Rate (m³/h) Heat Transfer Coefficient (W/m²K) and Nusselt Number.

Model Viscous	**Power of Combustion (kW)**	**Maximum Wall Temperature (K)**	***Air Volumetric Flow Rate* (m³/h).**	**Nusselt Number**	**Coefficient of Heat Transfer (W/m²K)**
Standard	200	1507	258.660	740.01	3.84
SST	200	1481	237.640	724.10	3.76
GEKO	200	1468	217.370	716.14	3.72
BSL	200	1445	205.560	702.06	3.64
Standard	700	1564	749.860	2712.18	14.08
SST	700	1548	728.810	2677.89	13.90
GEKO	700	1514	707.820	2605.05	13.52
BSL	700	1503	696.750	2581.48	13.40
Standard	1000	1614	1072.324	4027.58	20.90
SST	1000	1598	1051.302	3978.61	20.65
GEKO	1000	1562	1031.317	3868.42	20.08
BSL	1000	1551	1012.228	3834.75	19.90



(a) Pressure Distribution Contours

(b) Contour Distribution of Fluid Flow Streamlines

Fig. 6. (a) Pressure Distribution Contours and (b) Contour Distribution of Fluid Flow Streamlines on a Gas-Fired Industrial Burner Pyrolysis in Various Viscous k-ω Models with a Combustion Power Variation of 200 kW.

The fluid with low velocity enters the inlet of the pyrolysis gas-fired industrial burner and progressively flows into the burner and combustion chamber. The fluid flow subsequently evolves at a controlled velocity around the burner geometry. However, the fluid flow increases significantly by approximately 2 m/s when approaching the outlet due to the difference in cross-sectional area. This phenomenon results in a reduction of pressure, an elevation in viscosity, and a modification in flow behavior, which can be affected by variables including fluid viscosity, temperature, and the characteristics of the flow system. The flow pattern exhibits stability when traversing the outlet boundary conditions; however, this stability is not observed as the fluid enters the inlet domain and moves through the burner and combustion chamber. The flow rate significantly influences the overall performance of the pyrolysis gas-fired industrial burner system, encompassing distillate capacity, heat exchanger effectiveness, and fluid circulation. Grasping this effect is essential because of its influence on system analysis and flow characteristics, particularly in different combustion power scenarios.

4 Conclusion

This numerical analysis shows that the k-ω standard viscous model works best for pyrolysis gas-fired industrial burners, especially when the combustion power changes by 1000 kW. The study findings demonstrate that this model exhibits elevated values of air volumetric flow rate, maximum wall temperature, heat transfer coefficient, and Nusselt number. Consequently, employing the k-ω standard model can enhance the efficiency and productivity of the combustion process, facilitating the advancement of more sophisticated and sustainable combustion technology. The findings of this study may serve as a reference for the development of more efficient and environmentally sustainable pyrolysis gas-fired industrial burners, applicable across diverse industries employing combustion technology.

The authors would like to express their sincere gratitude to the Research and Community Service Center, Jakarta State Polytechnic, for providing support and facilities during the conduct of this research. This research was funded by P3M under the HIBAH-PIT 2025 scheme with contract number 819/PL3.A.10/PT.00.06/2025. The authors declare that the data in this paper do not plagiarize any articles. The contributions of each author are as follows: B. S. Rahayu Purwanti designed the research and analyzed the data, Rouf Muhammad conducted the simulation data collection, Hamid Ramadhan Nur wrote and revised the article, and Ghani Putra Nuari and Muhammad Fajar Ramadhan designed the tool drawings.

References

1. J. L. H. P. Sallevelt, A. K. Pozarlik, G. Brem, Numerical study of pyrolysis oil combustion in an industrial gas turbine. E. Conver. Management. **127**, 504–514 (2016). https://10.1016/j.enconman.2016.09.029
2. Y. Feng, Y. Jiang, X. Li, S. Zhang, J. Qin, Y. Cao, H. Huang, Numerical study on the influences of heat and mass transfers on the pyrolysis of hydrocarbon fuel in mini-channel. Appl. Therm. Engineering. **119**, 650–658 (2017). https://10.1016/j.applthermaleng.2017.03.010
3. G. Xu, L. Zang, P. Schwarz, H. Yang, Achieving China's carbon neutrality goal by economic growth rate adjustment and low-carbon energy structure. E. Policy. **183**, 113817 (2023). https://10.1016/j.enpol.2023.113817
4. Y. Song, X. Xian, C. Zhang, F. Zhu, B. Yu, J. Liu, Residual municipal solid waste to energy under carbon neutrality: Challenges and perspectives for China, R. Conserv. Recycling. **198**, 107177 (2023). https://10.1016/j.resconrec.2023.107177

5. I. M. Lawal, A. Ndagi, A. Mohammed, Proximate analysis of waste-to-energy potential of municipal solid waste for sustainable renewable energy generation. A. S. Eng. Journal. **15**, 102357 (2024). https://10.1016/j.asej.2023.102357
6. G. Mancini, L. Lombardi, A. Luciano, D. Bolzonella, P. Viotti, D. Fino, A reduction in global impacts through a waste-wastewater-energy nexus: A life cycle assessment, Energy. **289**, 130020 (2024). https://10.1016/j.energy.2023.130020
7. X. Liang, T. A. Kurniawan, H. H. Goh, Conversion of landfilled waste-to-electricity (WTE) for energy efficiency improvement in Shenzhen (China): A strategy to contribute to resource recovery of unused methane for generating renewable energy on-site. J. C. Production. **369**, 133078 (2022). https://10.1016/j.jclepro.2022.133078
8. F. Li, X. He, C. A. Shoemaker, C. H. Wang, Experimental and numerical study of biomass catalytic pyrolysis using Ni2P-loaded zeolite: Product distribution, characterization and overall benefit. E. C. Managament. **208**, 112581 (2020). https://10.1016/j.enconman.2020.112581
9. D. Csemány, D. Füzesi, V. Józsa, Numerical analysis on the thermal load and NO emission of a novel 1 MW pyrolysis gas/natural gas-fired industrial burner. Results Eng., **25**, 104388 (2025). https://10.1016/j.rineng.2025.104388
10. X. Mao, L. Li, M. Xu, Optimization and scale-up of methyl ricinoleate pyrolysis reactor: A numerical simulation and experimental study. A. Therm. Engineering. **274**, 126705 (2025). https://10.1016/j.applthermaleng.2025.126705
11. V. S. Dadi, S. Veluru, H. K. Taneru, Recent advancements of CFD and heat transfer studies in pyrolysis: A review. J. Anal. Appl. Pyrolysis, **175**, 106163 (2023). https://10.1016/j.jaap.2023.106163
12. M. Ren, R. Tan, J. Zhao, Experimental and numerical study on oxy-fuel combustion of pyrolysis gas at ultra-rich conditions with non-premixed and partially premixed nozzles. Int. J. Hydrogen Energy, **91**, 63–72 (2024). https://10.1016/j.ijhydene.2024.10.118
13. L. Chen, S. Pannala, B. Nair, Experimental and numerical study of a two-stage natural gas combustion pyrolysis reactor for acetylene production: The role of delayed mixing. P. C. Institute. **37**, 5715–5722 (2019). https://10.1016/j.proci.2018.05.170
14. H. Yu, H. Sun, S. Yang, G. Bao, H. Wang, Numerical simulation study of impact of polydispersity on biomass pyrolysis in draft-tube spouted reactor with fountain confiner. R. Energy, **223**, 120068 (2024), https://10.1016/j.renene.2024.120068
15. C. Wu, Y. Zhuo, X. Xu, An integrated experimental and numerical study of iron-coke briquettes' pyrolysis and reduction behaviour in an industrial-scale pyrolyser. P. Technology. **409**, 117822 (2022). https://10.1016/j.powtec.2022.117822